

Optimization of Closure Law of Guide Vanes for an Operational Hydropower Plant of Nepal

Saroj Chalise¹ and Dr. Laxman Poudel²

¹Student, Department of Mechanical Engineering, IOE Pulchowk Campus, NEPAL

²Professor, Department of Mechanical engineering, IOE Pulchowk Campus, NEPAL

¹Corresponding Author: chalisesaroj639@gmail.com

ABSTRACT

This paper addresses the optimization of two-stage closure law of guide vanes in an operational hydropower plant of Nepal. The mathematical model has been established in commercial software Bentley Hammer, whose correctness has been validated by comparing the results with the data of experimental load rejection test. The validated mathematical model has been employed to find the parameters of optimum closure pattern, which minimizes the non-linear objective function of maximum water pressure and maximum rotational speed of turbine.

Keywords— Guide Vanes, Closure Law, Optimization, Non-Linear Objective Function, Hydropower

I. INTRODUCTION

A. Background

In an operating hydropower plant, load rejection occurs in any of the cases, whenever the power generated by it is unable to be evacuated to the national grid. The rotational speed of the turbine rises soon after the load rejection [4]; hence, the guide vanes of a Francis turbine should be closed fast enough to prevent the rotating components from excessive rotational speed. However, the sudden closure of the guide vanes creates the hydraulic transient condition in the waterway network located upstream and downstream of the turbine [2]. During transient condition, water pressure fluctuates from maximum to minimum value in the entire water conduit, which if not designed carefully, can pose the risk of either bursting due to extremely high pressure or the cavitation due to extremely low pressure in the different sections of the pipe [2].

Various strategies can be implemented to the hydropower project to ensure the safe operation from the perspective of controlled values of pressure and rotational speed. This includes installation of surge chamber, installation of pressure relief valves, selection of penstock pipe having low Young's Modulus of Elasticity (E), addition of flywheel weight to increase the moment of

inertia (GD^2) of the rotating components and so on [1, 4, 6]. However, compared to these options, variation of the closure law of guide vane is the most economical option, since the closure law can be modified from the governor without the installation any new equipment in the system [4, 5, 9].

The closure law of guide vane can be linear, curved or the broken line with various stages. Considering the reliability in operation, the curved closure law is rarely used and the broken line closure patterns usually have less than three stages and hence, the two-stage closure law is the most preferred closure pattern for the designer [4].

Currently, there has been plenty of research on the effect of the closure law of guide vane and its optimization. Sheng et al. [4] studied the effect of the individual variation of different parameters of two-stage closure parameter on the maximum pressure and rotational speed. Zhao et al. [10] used the linear objective function to harmonize the contradiction of maximum pressure and maximum speed for a two-stage closure pattern. They also found that for a medium head hydropower plant, "slow after fast" is better option to control the pressure and speed rises, compared to "fast after slow" in a two-stage closure pattern. Li et al. [9] proposed an asynchronous closure of the different wicket gates to control the maximum pressure at the spiral casing. Zhou et al. [11] used simulated annealing algorithm to find the optimum parameters of closure pattern. The research on optimization of closure law and the effect of closure law on the various target parameters (Maximum pressure, minimum pressure and Maximum rotational speed) are abundant. However, very limited research has focused on the objective function of the optimization. The traditional linear objective function can ensure the target parameters within the permitted scope [9]. However, unlike non-linear objective function; it does not guarantee the better distribution of the safety margin of each target [5]. Hence, this paper focuses on the optimization of the parameters of a two-stage closure pattern for a typical operational plant of Nepal using non-linear objective function of pressure and speed rise.

B. Mathematical Modeling

The momentum and continuity equations for unsteady flow in the pressurized pipeline have been expressed in equation 1 and equation 2 [2].

$$\frac{\partial V}{\partial t} + \frac{1}{\rho} \frac{\partial}{\partial x} + \frac{fV|V|}{2D} = 0. \quad \dots(1)$$

$$\frac{\partial P}{\partial t} + \rho c^2 \frac{\partial V}{\partial x} = 0 \quad \dots(2)$$

Where,

- P = Pressure,
- V = Flow velocity
- f = Darcy Weisbach friction factor
- c = Wave speed
- ρ = Density of fluid
- D = Diameter
- x = Co-ordinate along the longitudinal section of the pipe

Equation 1 and 2 represents a pair of quasi-static hyperbolic partial differential equations. Although the general solution is not possible to these equations, these equations can be transferred to ordinary differential equations using Methods of Characteristics and then integrated within limits to obtain the solution within defined co-ordinate of space and time. The value of pressure and velocity at *i*th node and *j*th time step can be calculated numerically using equation 3 and equation 4 [3].

$$P_{i,j} = \frac{1}{2}(P_{i-1,j-1} + P_{i+1,j-1}) + \frac{\rho c}{2}(V_{i-1,j-1} - V_{i+1,j-1}) - \frac{\rho c}{2} \left(\frac{fc}{2D} \Delta x |V_{i-1,j-1}| + \frac{fc}{2D} \Delta x V_{i-1,j-1} |V_{i+1,j-1}| \right) \quad \dots(3)$$

$$V_{i,j} = \frac{1}{2} \frac{1}{\rho c} (P_{i-1,j-1} - P_{i+1,j-1}) + \frac{1}{2} (V_{i-1,j-1} + V_{i+1,j-1}) + \frac{1}{2} \left(\frac{fc}{2D} \Delta x V_{i+1,j-1} |V_{i+1,j-1}| - \frac{fc}{2D} \Delta x V_{i-1,j-1} |V_{i-1,j-1}| \right) \quad \dots(4)$$

Equation 3 and 4 contains the term acoustic wave velocity, which has been calculated using the Kortweg’s equation. The Kortweg’s equation for wave speed (c), in the pipe having thickness e, Diameter D, support factor Ψ and Young’s modulus *E_v* is expressed in the equation 5 [7].

$$c = \sqrt{\frac{E_v}{\rho(1 + \frac{DE}{eE} \Psi)}} \quad \dots(5)$$

Where, *E* and ρ are the bulk modulus and the density of the fluid. Equation 3, equation 4 and equation 5 are used in combination to find the velocity and pressure at any co-ordinate of time and space. The rise of rotational speed of turbine has been governed by equation 6.

$$I \frac{d\omega}{dt} = M_h - M_g \quad \dots(6)$$

Where,

- I* = Polar moment of inertia of the rotating parts in turbine-generator combination
- ω = Angular speed the turbine
- M_h* = Torque from the water that is spinning the turbine
- M_g* = Torque from the generator that the turbine is connected to

By solving the equation 6, combined with the turbine characteristics curve and equation 3 and equation 4, the unknown parameter at turbine node at any instant can be found out.

II. METHODOLOGY

A. Numerical Model Development and Validation

The numerical model has been developed for a typical medium head hydropower plant of Nepal in commercial software BENTLEY HAMMER, which uses Method of Characteristics to solve the governing equation of momentum and continuity for unsteady flow in the conduit. The schematics of the waterway diagram of the hydropower plant have been shown in figure 1.

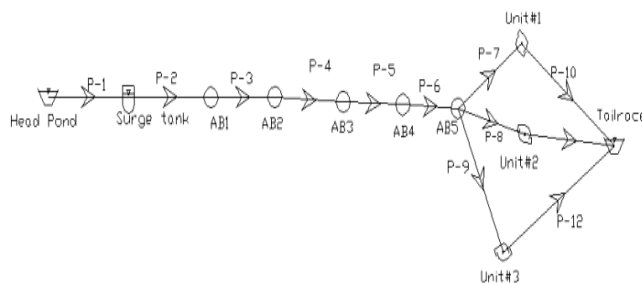


Figure 1: Schematics of waterway diagram

TABLE I
DIMENSION DETAILS OF WATERWAY DIAGRAM

Pipe Section	Length (m)	Diameter (mm)	Start node-elevation (m)	Stop-node elevation (m)
P1	2200	3500	320.5	316
P2	47	2600	316	288
P3	80	2600	288	262
P4	82	2600	262	240
P5	20	2000	240	232
P6	22	1800	232	216
P7	8	1500	216	198
P8	3	1500	216	198
P9	8	1500	216	198
P10	8	1500	198	196
P11	3	1500	198	196
P12	3	1500	198	196

The hydropower station has three units, each having an installed capacity of 7.5 MW. The net head and net flow of each turbine is 108.23 meter and 24cubic meters per second. The rated rotational speed of the generator is 600 RPM and the rotating system has a combined moment of inertia of 31,000 kg.m².

The friction model is assumed to be quasi-static and the time steps has been kept 0.005 seconds for computation. The number of computational reach has been adjusted through the software Bentley Hammer to keep the Courant-Friedrichs -Lewy Number, (cΔt/Δx), equals to one to match the computational compliance criteria [8]. The wave speed is calculated by using Korteweg’s equation. The computation has been done for the 3000 second time soon after the wicket gate closure is started.

The numerical simulation has been done for the same closure pattern as did experimentally during the load rejection test, which was carried out during the commissioning phase of the project. The validation of the developed numerical model has been done by comparing the maximum value of pressure and rotational speed of the turbine as obtained from numerical simulations with the data of the load rejection test. The numerical model after validation has proved to be reliable for further operation and hence the model has been applied to find the optimum closure pattern of the guide vanes.

B. Optimization Variables

The optimization variables are four free parameters describing the two-stage closure pattern as shown in figure 2; time at which first closure stage finishes (t1), time at which second stage closure starts (t2), the fold point position (s) and the time at which the wicket gates are fully closed (t3).

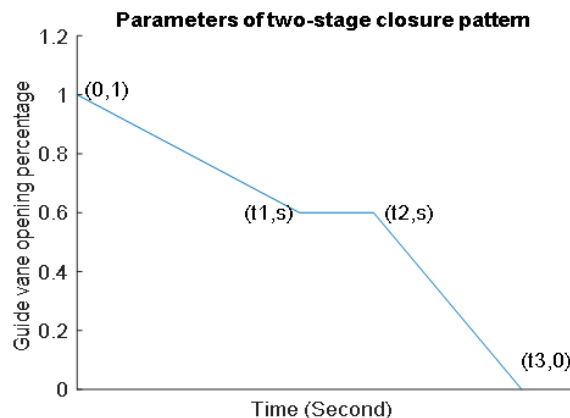


Figure 2: Optimization variables

C. Objective Function

For the optimization, a non-linear objective function has been defined as follows:

$$F = \frac{N_a - N_i}{N_a - N_{max}} \cdot \frac{P_a - P_i}{P_a - P_{max}}, \text{ if } N_{max} < N_a \text{ and } P_{max} < P_a$$

$$F = \infty, \text{ if } N_{max} > N_a \text{ OR } P_{max} > P_a$$

$$\text{And SF} = \frac{P_a}{P_{max}} \cdot \frac{N_a}{N_{max}}$$

Where

- N_a = Allowable maximum rotational speed of turbine
- N_{max} = Maximum rotational speed
- N_i = Rotational speed at initial steady state
- P_a = Maximum allowable pressure
- P_{max} = Maximum pressure
- P_i = Pressure at initial steady state
- SF = Overall safety factor of the system

The denominator of the objective function contains the product of two terms, each representing the difference of the maximum and allowable value of each sub-goal. Hence, it is supposed that the optimum solution based on this objective function will uniformly distribute the safety margin of each objective goal compared to the conventional linear objective function.

The value of initial steady-state pressure has been calculated by using a steady-state solver of Bentley hammer software. For the consideration of safety, the maximum allowable values of speed and pressure are set as N_a = 900 RPM and P_a = 1800 KPA.

D. Optimization Algorithm

The numerical simulation has been repeatedly done by varying one variable at once. The t_2 and t_1 have been related by the defined relationship. The remaining three variables; t_1 , t_3 and s , each has been provided five variations over the uniform interval, accounting for a total of one hundred and twenty-five combinations of t_1, t_2, t_3 and s . The value of maximum pressure and maximum rotational speed calculated for each combination are used to evaluate the objective function. The combination of t_1, t_2, t_3 and s which gives the minimum value of the objective function has been considered as optimum parameters for a two-stage closure pattern. The overall safety factor has been calculated and compared with the value of the objective function.

III. RESULTS

A. Numerical Model Development and Validation

The data of experimental load rejection test suggests that for the full rejection of load, the closure pattern was single-stage linear and the closure time was varied by rotating the knob of a throttle valve of the governor. The four variations in closure period were five ten, fifteen and twenty seconds as shown in figure 3.

The results of numerical simulation for the single-stage linear closure pattern with closure period $t = 5$ seconds, has been shown in Figure 4, 5, 6 and 7. The spatial variation of pressure along the longitudinal section of penstock pipe considering the start of the spiral casing as $x=0$ has been shown in figure 4. The red, green and blue lines in the figure indicates maximum, initial and minimum pressures respectively. The figure shows that the maximum pressure is observed at the start of the spiral casing. The temporal variation of the pressure at the same position has been shown in figure 5. The result shows that the pressure increases steeply till the time $t = 5$ seconds and fluctuation starts. The fluctuation gradually dampens which has been shown in figure 6. From figure 3 and figure 5, it can be seen that the value of maximum pressure along the entire pipeline is 1722 KPA which is observed on start of spiral casing at time $t = 13$ second. Figure 7 shows the temporal variation of the rotational speed of the turbine for closure time $t = 5$ seconds. The result shows that speed rises rapidly soon after the load rejection. The maximum value of the rotational speed is 722 RPM.

The numerical simulation has been repeated for the single-stage linear closure pattern with different closure periods of 10, 15 and 20 seconds. The value of maximum pressure and maximum rotational has been summarized in table II. The comparison of numerical and experimental results is shown in figure 8. The figure shows that numerical simulations show satisfactory agreement with the data of field test on the premise of an identical pattern of the

closure of wicket gates. The maximum deviation of the numerical and experimental result is found to be 3%.

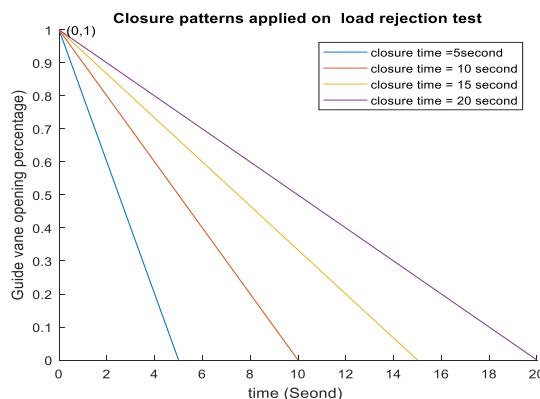


Figure 3: Various closure patterns applied for experimental load rejection test

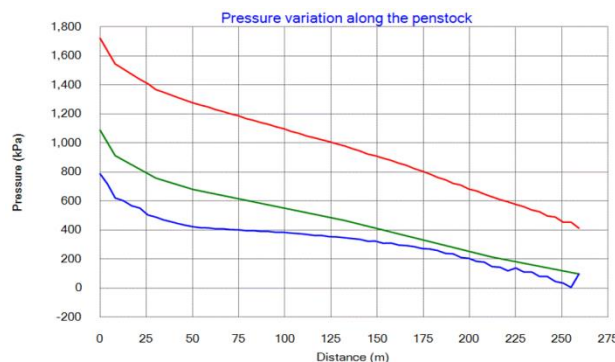


Figure 4: Pressure variation along the longitudinal section of the penstock profile

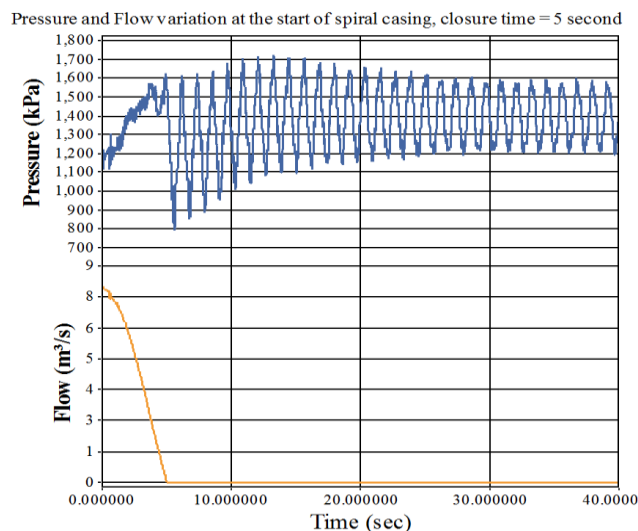


Figure 5: Temporal variation of pressure and flow at the start of spiral casing for closure time, $t = 5$ second

Pressure at start of spiral casing, closure time = 5 second

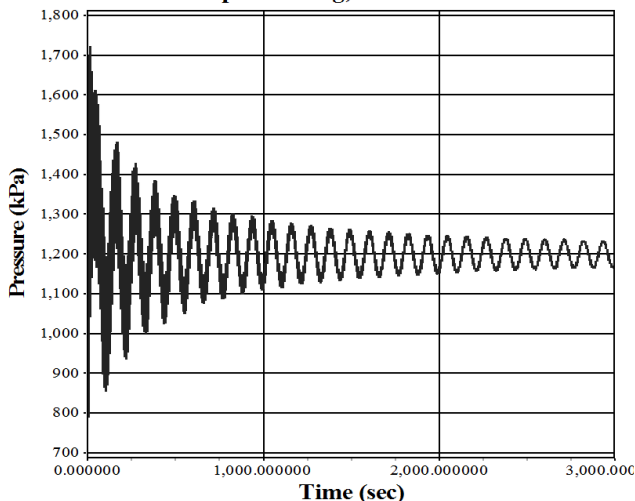


Figure 6: Temporal variation of pressure at the start of spiral casing for closure time, t= 5 second

Temporal variation of rotational speed of turbine

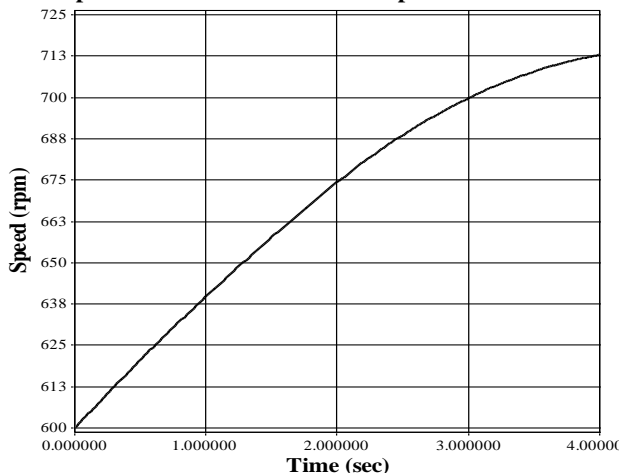


Figure 7: Temporal variation of the rotational speed of runner for closure time of 5 second

TABLE II
SUMMARY OF RESULTS OF NUMERICAL SIMULATIONS FOR SINGLE-STAGE LINEAR CLOSURE PERIOD

Closure time (second)	5	10	15	20
Maximum Pressure (KPA)	1722	1580	1525	1496
Maximum Speed (RPM)	722	792	845	886

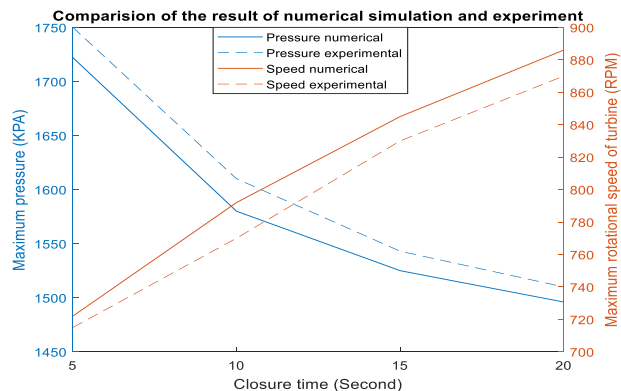


Figure 8: Comparison of results of numerical simulation with the experiment

B. Optimization of the closure pattern

The results of numerical simulations for a different combination of the four optimization variables t1, t2, t3, and s have been presented in Table III.

TABLE III
RESULT OF NUMERICAL SIMULATION FOR VARIOUS COMBINATIONS OF PARAMETER OF TWO-STAGE CLOSURE PATTERN

Closure Law [t1,t2,t3,s]	Maximum pressure (Kpa)	Maximum Rotational speed of turbine (RPM)	Objective function
[6, 7, 21,0.2]	1567	759	7.305
[6, 7, 21,0.35]	1480	816	8.929
[6, 7, 21,0.5]	1488	859	18.762
[6, 7, 21,0.65]	1503	888	67.340
[6, 7, 21,0.8]	1490	909	infinity
[7.3, 8.8, 21,0.2]	1552	780	8.065
[7.3, 8.8, 21,0.35]	1487	834	11.618
[7.3, 8.8, 21,0.5]	1492	874	29.970
[7.3, 8.8, 21,0.65]	1486	900	infinity
[7.3, 8.8, 21,0.8]	1521	919	infinity
[8.5, 10.5, 21,0.2]	1529	799	8.768
[8.5, 10.5,21,0.35]	1488	849	15.083
[8.5, 10.5, 21,0.5]	1510	887	63.660
[8.5, 10.5,21,0.65]	1509	911	infinity
[8.5, 10.5, 21,0.8]	1509	928	infinity
[9.8, 12.3, 21,0.2]	1499	817	9.607

[9.8, 12.3,21,0.35]	1490	864	21.505
[9.8, 12.3, 21,0.5]	1488	900	infinity
[9.8, 12.3,21,0.65]	1513	922	infinity
[9.8, 12.3, 21,0.8]	1522	937	infinity
[11, 14, 21,0.2]	1552	833	14.444
[11, 14, 21,0.35]	1496	877	34.325
[11, 14, 21,0.5]	1534	912	infinity
[11, 14, 21,0.65]	1526	932	infinity
[11, 14, 21,0.8]	1591	946	infinity
[9, 12, 18,0.35]	1482	853	16.058
[9, 12, 18,0.5]	1489	889	70.155
[9, 12, 18,0.65]	1594	911	infinity
[9, 12, 18,0.8]	1555	926	infinity
[5, 6, 18,0.65]	1487	866	22.552
[5, 6, 18,0.8]	1529	888	73.801
[6, 7.5, 18,0.2]	1600	759	8.511
[6, 7.5, 18,0.35]	1485	811	8.561
[6, 7.5, 18,0.5]	1500	851	16.327
[6, 7.5, 18,0.65]	1495	878	35.768
[6, 7.5, 18,0.8]	1514	898	419.580
[7, 9, 18,0.2]	1566	776	8.271
[7, 9, 18,0.35]	1486	826	10.329
[7, 9, 18,0.5]	1482	864	20.964
[7, 9, 18,0.65]	1525	890	87.273
[7, 9, 18,0.8]	1508	908	infinity
[8, 10.5, 18,0.2]	1517	792	7.852
[8,10.5,18,0.35]	1496	840	13.158
[8, 10.5, 18,0.5]	1524	877	37.807
[8,10.5,18,0.65]	1497	901	infinity
[8, 10.5, 18,0.8]	1587	917	infinity
[9, 12, 18,0.2]	1543	806	9.935
[8, 10.5,15,0.2]	1528	792	8.170
[8, 10.5,15,0.35]	1527	834	13.320
[8, 10.5, 15,0.5]	1592	867	34.965
[8, 10.5, 15,0.65]	1550	889	87.273
[8, 10.5, 15,0.8]	1648	905	infinity
[2, 3, 12,0.2]	2061	674	infinity
[2, 3, 12,0.35]	1717	726	16.618
[2, 3, 12,0.5]	1544	766	6.996
[2, 3, 12,0.65]	1524	797	8.442

[2, 3, 12,0.8]	1507	820	10.239
[4, 5, 12,0.2]	1656	721	9.311
[4, 5, 12,0.35]	1503	763	5.898
[4, 5, 12,0.5]	1526	796	8.422
[4, 5, 12,0.65]	1520	821	10.850
[4, 5, 12,0.8]	1583	841	18.746
[6, 7, 12,0.2]	1570	759	7.401
[6, 7, 12,0.35]	1524	794	8.203
[6, 7, 12,0.5]	1564	823	13.207
[6, 7, 12,0.65]	1542	844	16.611
[6, 7, 12,0.8]	1575	861	27.350
[7, 8, 12,0.2]	1520	776	6.912
[7, 8, 12,0.35]	1509	808	8.965
[7, 8, 12,0.5]	1556	835	15.132
[7, 8, 12,0.65]	1593	855	25.765
[7, 8, 12,0.8]	1747	870	150.943
[9, 10, 12,0.2]	1542	806	9.896
[9, 10, 12,0.35]	1692	834	33.670
[9, 10, 12,0.5]	1812	857	infinity
[9, 10, 12,0.65]	1873	873	infinity
[9, 10, 12,0.8]	2083	885	infinity
[2, 3, 9,0.2]	2093	674	infinity
[2, 3, 9,0.35]	1717	716	15.715
[2, 3, 9,0.5]	1544	748	6.168
[2, 3, 9,0.65]	1580	773	8.590
[2, 3, 9,0.8]	1534	793	8.432
[3, 4, 9,0.2]	1847	699	infinity
[3, 4, 9,0.35]	1547	736	5.784
[3, 4, 9,0.5]	1566	765	7.597
[3, 4, 9,0.65]	1536	787	8.045
[3, 4, 9,0.8]	1574	805	11.178
[4, 5, 9,0.2]	1660	721	9.577
[4, 5, 9,0.35]	1507	754	5.610
[4, 5, 9,0.5]	1540	780	7.692
[4, 5, 9,0.65]	1595	801	11.826
[4, 5, 9,0.8]	1734	816	43.290
[5, 6, 9,0.2]	1559	741	6.263
[5, 6, 9,0.35]	1573	771	8.196
[5, 6, 9,0.5]	1618	795	12.559
[5, 6, 9,0.65]	1756	813	62.696

[5, 6, 9,0.8]	1762	827	86.518
[6, 7, 9,0.2]	1537	759	6.472
[6, 7, 9,0.35]	1681	787	17.848
[6, 7, 9,0.5]	1761	809	67.625
[6, 7, 9,0.65]	1852	825	infinity
[6, 7, 9,0.8]	2054	837	infinity

*Note: [6, 7, 21, 0.2] means $t_1=6$ second, $t_2=7$ second, $t_3=21$ second and $s=0.2$

The optimized value of t_1 , t_2 , t_3 , and s , based on one hundred and twenty-five simulations are 4 seconds, 5 seconds, 9 seconds, and 0.35 respectively. The corresponding values of the maximum pressure, maximum rotational speed and the objective function are 1507 KPa, 754 RPM, and 5.61 respectively.

IV. CONCLUSION

This article deals with the development of mathematical model of hydraulic transients for a typical medium head hydropower plant. The correctness of results of the mathematical model has been validated in comparison with the experimental data. The maximum deviation of the numerical and experimental result has found to be 3%, which concludes that the numerical model can predict the parameters of hydraulic transient with satisfactory accuracy.

Moreover, the article focuses on the optimization of two-stage closure pattern of guide vanes with non-linear objective function of two sub-goals. The optimized parameters have effectively harmonized the contradiction of rise of hydrodynamic pressure and rotational speed, ensuring both the target parameters within the permitted scope. The overall safety factor for the optimum solution is 1.425. The achievement of this study can be a reference for similar projects.

REFERENCES

- [1] A Bergant, B Karney, S Pejovic, & J Mazij, ed. (2014). Treatise on water hammer in hydropower standard and guidelines. *IOP Conference Series: Earth and Environmental Science*, 22(4). DOI: 10.1088/1755-1315/22/4/042007.
- [2] Benjamin Wylie, Lisheng Suo, & Victor LStreeter. (1993). *Fluid transients in systems*. Englewood Cliff: Prentice Hall.
- [3] Carlsson, Joel. (2016). *Water hammer phenomenon analysis using the method of characteristics and direct measurements using a "stripped" electromagnetic flow meter*. Available at: <http://www.diva-portal.org/smash/get/diva2:981316/FULLTEXT01.pdf>.
- [4] Chen Sheng, Jhan Jiang, & Yu xiaodong. (2013). Optimization of two stage closure law of wicket gate and application. *Applied Mechanics and materials*, 636-641.
- [5] Cui, H., Fan, H. Chen, N. "Optimization of wicket gate closing law considering different case. *IOP Conference series: Earth and Environmental Science*, 44(20), Reference Number: 44052853.
- [6] Sharif F, Siosemarde M, Merufinia E, & Esmat Saatlo M. (2014). Comparative hydraulic simulation of water hammer in transition pipe line systems with different diameter and types. *Journal of Civil Engineering and Urbanism*, 4(3), 282-286.
- [7] Tijsseling, A.S. (1996). Fluid-structure interaction in liquid filled pipe systems: A review. *Journal of Fluids and Structures*, 10(2), 109-146.
- [8] Urbanowicz, Kamil. (2017). Computational compliance criteria in water hammer modelling. *E3S Web of Conferences, International Conference Energy, Environment and Material Science*. EDP Sciences. Available at: <https://publications.edpsciences.org/>.
- [9] Xiaoqin Li, Jinshi Chang, & Peng Chen. (2013). Wicket gate closure control law to improve the transient of a water. *Advanced Material and Research*, 732(33), 451-456.
- [10] Weiguo Zhao, Liying Wang, Ziyong Zhai, Zijun Wang. (2010) Application of multi-objective optimized methods in the closing law of guide vanes. *Chinese Control and Decision Conference* 3552-3556.
- [11] Zhou T, Zhang J., Yu, X, & Chu, S. (2018). Optimizing closure law of wicket gates in hydraulic turbine based on simulated annealing. *Journal of Drainage and Irrigation Machinery Engineering*, 36, 320-326.